

SLOSHING IN A T-BAFFLED RECTANGULAR STORAGE TANK NUMERICAL STUDY FOR 2-D PROBLEMS

Hakan AKYILDIZ*

* *İstanbul Teknik Üniversitesi*

ABSTRACT

The liquid sloshing in a moving partially filled rectangular tank with vertical and T-shape baffles is investigated. A numerical algorithm based on the volume of fluid technique (VOF) is used to study the non-linear behaviour of liquid sloshing. The numerical model solves the complete Navier-Stokes equations in primitive variables by using of finite difference approximations with the moving coordinate system. The ratio of the baffle height to the initial liquid depth has been changed in the range of $0 \leq h_B / h \leq 1.0$. The effect of the T-shape baffle and vertical baffle height to reach the roof of the tank have been investigated. It is observed that a vertical baffle for $h_B / h < 0.8$ would be more effective except the maximum dynamic pressure at T2 and T-shape baffle having a height $h_B / h \geq 0.8$ would be very effective in reducing the dynamic pressure. On the other hand, the maximum overturning moment for the T-baffled case would be much smaller. In order to assess the accuracy of the method used, some results with vertical baffle are compared with the available experimental results. The time variations of pressures have been also presented.

Keywords: Sloshing, Two-dimensional free surface flow, Volume of fluid technique, Finite difference method, T-Baffle

1. Introduction

Liquid sloshing in a moving tank constitutes major components in a number of dynamical systems such as aerospace vehicles, road tankers, liquefied natural gas carriers, elevated water towers and petroleum cylindrical tanks. Fluid motion in partially filled tanks can cause large structural loads if the period of tank motion is close to the natural period of fluid inside the tank (Ibrahim, 2005; Faltinsen and Timokha, 2009). The amplitude of the slosh, in general, depends on amplitude and frequency of the tank motion, liquid-fill depth, liquid properties and tank geometry. These parameters have direct effects on the dynamic stability and performance of moving tanks. The baffle inside a tank has investigated many researchers and the several recent studies on the effect of baffle on liquid sloshing are summarized as follows.

There has been a considerable amount of work on liquid sloshing. Some of these studies are reported by Ibrahim et al. (2001), Faltinsen and Timokha (2001). Faltinsen and Timokha, (2001) analysed the two-dimensional nonlinear sloshing of an incompressible fluid with irrotational flow in a rectangular tank by a modal theory. The theory they used is in good agreement with experimental results but the model assumes infinite tank roof height.

Akyildiz and Unal (2005; 2006) investigated the pressure variations in both baffled and unbaffled rectangular tank numerically and experimentally. They observed that the effects of the

vertical baffle are most pronounced in shallow water and consequently the pressure response is reduced by using the baffles. When an internal element is put into a tank, the liquid viscosity cannot be neglected and energy is dissipated by viscous action. Celebi and Akyildiz (2002) revealed that flow over a vertical baffle produces a shear layer and energy is dissipated by viscous action. They concluded that, in an increased fill depth; the rolling amplitude and frequency of the tank with or without baffle configurations directly affect the degrees of non-linearity of the sloshing phenomena. As a result of this, a phase shift in forces and moments occurred.

Kim (2001) analysed the sloshing flows with impact load in the two and three-dimensional containers based on a finite difference method. In this study, the Navier-Stokes equation with free boundary was solved using the SOLA scheme and the free surface profile was assumed to be a single-valued function. Armenio and La Rocca (1996) adopted the finite difference method to solve the 2D RANS equations to overcome the strong interaction between vorticity and free surface motion. The control of the sloshing behaviour with baffles is also a subject of interest in the recent years, because of the complexity and highly non-linear nature of the problem. Some researches carried out the experimental and numerical studies and pointed out the above mentioned characteristics (Akyildiz and Unal, 2006; Panigrahy et al., 2009; Pal et al., 2002; Sames et al., 2002).

Cho and Lee (2004) denoted that the liquid motion and the dynamic pressure distribution above the baffle are more active than those below the baffle by carrying out the parametric study on two-dimensional liquid sloshing. They used the baffled tank under forced horizontal excitation considering potential flow theory. Cho et al. (2005) carried out a numerical method to analyze the resonance characteristics of liquid sloshing in a 2D baffled tank. They cannot resolve the viscous and the rotational motion of the liquid sloshing because of the potential flow theory. Pal and Bhattacharyya (2010) carried out the numerical and experimental studies of liquid sloshing for 2-D problem. The resulting slosh heights for various excitation frequencies and amplitudes are compared with the data obtained numerically. It was concluded that the little variations in the data are due to the ineptness of the experimental set up and the input parameters. Younes et al. (2007) investigated the hydrodynamic damping experimentally in rectangular tanks with vertical baffles of different heights and numbers. It is pointed out that the damping ratio increases by increasing the baffle numbers.

Liu and Lin (2009) studies 3D liquid sloshing in a tank with baffles using the numerical approach. They showed that the vertical baffle is more effective than the horizontal baffle in reducing the amplitude and the pressure on the wall. The commercial CFD code has been utilized to investigate the liquid sloshing recently (Godderidge et al., 2006b, 2007; Godderidge et al., 2009a, 2009b). They showed good agreement with the experimental data.

In this study, the effects of the vertical baffle height and the horizontal baffles on liquid sloshing in a rolling rectangular tank have been investigated. Furthermore, it is examined that how the vortex resulting from the baffle tip affects the liquid sloshing and flow physics. A numerical algorithm based on the volume of fluid technique (VOF) is used to study the non-linear behaviour of liquid sloshing. The numerical model solves the complete Navier-Stokes equations in primitive variables by using of finite difference approximations with the moving coordinate system. It is difficult to analyse how flow physics such as the vortex from the baffle tip could be used to understand the effect of the baffle on liquid sloshing. Therefore, the main purpose of this study is to examine the behaviour of the tip vortex and to assess numerically

how the height of the baffle relative to the initial liquid depth with horizontal baffles affects liquid sloshing. The T-baffle is located at the center of the bottom of the tank. Thus, this study provides an investigation of the free surface elevation according to the baffles and the pressure distributions on the tank wall.

2. Mathematical formulation and numerical approach

The fluid is assumed to be homogenous, isotropic, viscous and Newtonian. Tank and fluid motions are assumed to be two-dimensional. The domain considered here is a rigid rectangular container partially filled with liquid, as shown in Fig. 1.

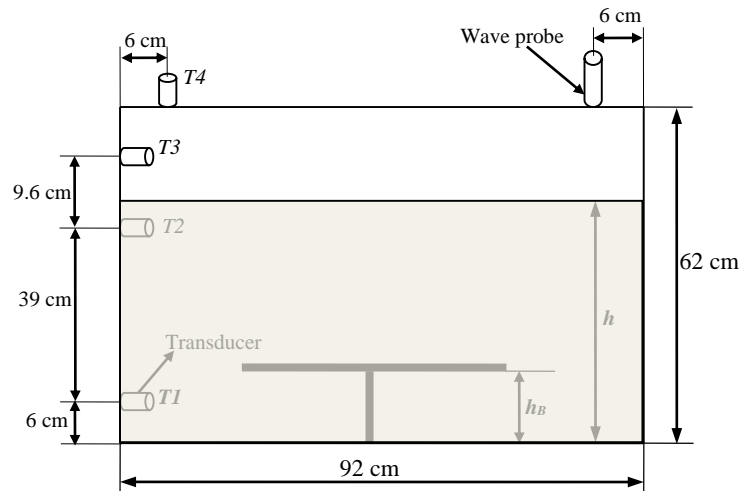


Figure 1. Schematic diagram of the pressure transducers and baffle configuration.

The governing equations are solved simultaneously with the corresponding boundary conditions and free surface kinematics and dynamic boundary conditions in the fluid domain.

$$\nabla \mathbf{U}(u, v) = 0 \tag{1}$$

$$\frac{\partial \mathbf{U}}{\partial t} + \mathbf{U} \cdot \nabla \mathbf{U} = -\frac{1}{\rho} \cdot \nabla \mathbf{P} + \mathbf{F} + \nu \nabla^2 \mathbf{U} \tag{2}$$

where $\mathbf{U}(u, v)$ is the velocity vector defined in the tank fixed coordinate and, ρ , P , ν and F are the liquid density, pressure, kinematic viscosity and external forces respectively.

In order to include the non-linearity and avoid the complex boundary conditions of moving walls, the moving coordinate system is used. The origin of the coordinate system is at the position of the center plane of the tank and on the undisturbed free surface. The moving coordinate is translating and rotating relative to an inertial system which can be used to represent general roll or pitch of the tank.

The external force consists of gravitational forces, the translational and rotational inertia forces, which can be written as,

$$\mathbf{F} = \mathbf{g} - \frac{d\mathbf{V}}{dt} - 2\boldsymbol{\Omega} \times \mathbf{V} - \frac{d\boldsymbol{\Omega}}{dt} \times \mathbf{r} - \boldsymbol{\Omega} \times (\boldsymbol{\Omega} \times \mathbf{r}) \quad (3)$$

where \mathbf{g} , \mathbf{V} and $\boldsymbol{\Omega}$ are the gravitational vector, the translational velocity and the rotational velocity vector. In addition, \vec{r} is the position vector of the considered point relative to O . On the free surface, both the kinematics and dynamic conditions should be satisfied:

$$\frac{\partial \eta}{\partial t} + \mathbf{U} \cdot \nabla (\eta - z) = 0 \quad (4)$$

$$P = P_{\text{atm}} \quad (5)$$

where η represents the free surface profile and P_{atm} is the air pressure or ullage pressure inside the tank. The surface tension is ignored in this study. Therefore, a no-shear is needed on the free surface. But, proper wall conditions are necessary on the tank walls and the internal members.

2.1 Numerical Computation

For the analysis of the sloshing flow inside a partial filled tank, a finite difference method is applied to the governing equations. A FDM (finite difference method) is useful when there are internal structures inside the tank or the fluid contacts the tank ceiling frequently. As the internal structures exist, the viscous effects may be dominant. In this study, the method concentrates on the global fluid motion, so some local effects, such as turbulence and wave breaking have been ignored. In some cases, these local effects are important, but the simulation of global flow plays a more critical role in many sloshing problems, due to the slosh-induced moment in the ship cargo (Kim, 2001).

The scheme adopted in this study is the SOLA method (Hirt and Nichols, 1981). Tank volume is discretized into Cartesian staggered grid cells. A single layer of fictitious cells (or boundary cells) surrounds the fluid region. The fictitious cells are used to set the boundary conditions so that the same difference equation can be used in the interior of the mesh (Lee et al., 2007; Liu and Lin, 2009; Eswaran et al., 2009).

Fluid velocities are located at the centers of the cell boundaries and pressure (P) and the volume of fluid function (F) are computed at the center of the cell. The solution algorithm works as a time cycle or 'movie frame'. The results of the time cycle act as initial conditions for the next one. At each step, suitable boundary conditions must be imposed at all boundaries.

There are two alternatives for the wall conditions; when the viscosity effect on the tank boundary is significant, the no-slip condition should be imposed. However, in most sloshing problems, the viscous effect is not significant and the boundary layer thickness is much less than the cell size. Therefore, the free slip condition is applied in the present study. For example, if the left boundary of the computing mesh is to be a rigid free slip wall, the normal velocity will be zero and the tangential velocity should have no normal gradients, i.e.

$$\begin{aligned} u_{1,j} &= 0 \\ v_{1,j} &= v_{2,j} \quad \text{for all } j \end{aligned} \tag{6}$$

2.2 Numerical Stability and Accuracy

Numerical calculations can have quantities that develop large, high frequency oscillations in space or time or both of them. This behaviour is usually referred to as a numerical instability. To prevent this type of numerical instability or inaccuracy, certain restrictions must be observed in defining the mesh increments Δx_i and Δy_j , the time increment Δt and the upstream differencing parameter α .

For accuracy, the mesh increments must be chosen small enough to resolve the expected spatial variations in all dependent variables. Once a mesh has been chosen, the choice of the time increment necessary for stability is governed by two restrictions. First, material cannot move through more than one cell in one time step, because the difference equations assume fluxes only between adjacent cells. Therefore, the time increment must satisfy the inequality,

$$\Delta t < \frac{\Delta(x, y)}{\Delta U_{i,j}} \quad \text{or,} \tag{7}$$

$$\Delta t < \text{Min} \left\{ \frac{\Delta x_i}{|u_{i,j}|}, \frac{\Delta y_j}{|v_{i,j}|} \right\} \tag{8}$$

where the minimum is with respect to every cell in the mesh. When a non-zero value of kinematic viscosity, momentum must not diffuse more than one cell in one time step. A linear stability analysis shows that this limitation implies,

$$\nu \Delta t < \frac{1}{2 \cdot (1/\Delta x_i^2 + 1/\Delta y_j^2)} \tag{9}$$

In this study, Δt is automatically chosen to satisfy the above inequalities. In order to insure the numerical stability, the parameter α is,

$$1 \geq \alpha \geq \text{Max} \left\{ \frac{u_{i,j} \cdot \Delta t}{\Delta x}, \frac{v_{i,j} \cdot \Delta t}{\Delta y} \right\} \tag{10}$$

2.3 Tank configuration

Fig. 1 denotes the 2D-rectangular tank with T-shape baffle and the locations of the transducers to obtain the pressure distributions with time (Akyildiz and Unal, 2006; Chen et al., 2009). For all cases, the fluid depth (h) is 75% of the tank height. The baffles are assumed to be rigid and

thin enough. The height of the baffle (h_B) is established by the ratio to liquid depth which varies from 0.2 to 1.0. The pressure transducers are installed on the left side in the center plane of the beam and one location on the top wall.

Present numerical code is set up to handle a simple harmonic forcing function. Thereafter, it advances the velocities in time explicitly using the two momentum equations. First, the angular displacement and its derivatives are calculated. The apparent acceleration terms are then calculated and finally the advective, diffusion and pressure gradients terms are calculated yielding an estimate of the velocity at the new time level. The tank motion is the pitch oscillations about y-axis only which follows the sinusoidal function given as where θ_0 and ω are the rolling amplitude and the frequency, respectively. The rolling amplitude is chosen as 40 and 80 in this study.

In order to testify and verify the discretization of the numerical model, three different grid systems are chosen for various fill depth (16×31 , 23×31 and 46×31) for the liquid fills 50% and 75% of the tank height. Generally, the choice of ' Δt ' is of extreme importance. In explicit schemes, ' Δt ' will govern the stability and also the accuracy, while in implicit schemes it will affect the accuracy. In this study, the value of ' Δt ' can be automatically calculated by the program and dynamically modified to insure stability and also optimize the pressure solution. When the excitation is harmonic rolling, it has been found that the normalized time step is somewhat independent of the forcing period. Therefore, about 200 time steps are required per forcing period in this program. This seems to hold regardless of discretization. A relatively fine discretization (46×31) with a finer enforcement of the velocity divergence requires three seconds of computer time per time step comparing a coarse discretization (16×31). Therefore, (46×31) grid system is chosen to obtain results in a reasonable time considering stability and accuracy. Furthermore, as the liquid responds violently increasing the period and the amplitude of the excitation, the numerical solution becomes unstable. So, for the sake of avoidance of the instability, the rolling amplitude is chosen as 40 to testify the grid dependence.

Fig. 2 and Fig. 3 show the reasonable agreement of the time variations of the pressure for different grid systems at T1 (50% liquid fill) and T3 (75% liquid fill). To estimate the limited impact pressure on the tank top and to demonstrate the capability of the numerical code in computing impact-type loads, the liquid sloshing at 75% fill depth with the rolling amplitude 80 are chosen for all cases.

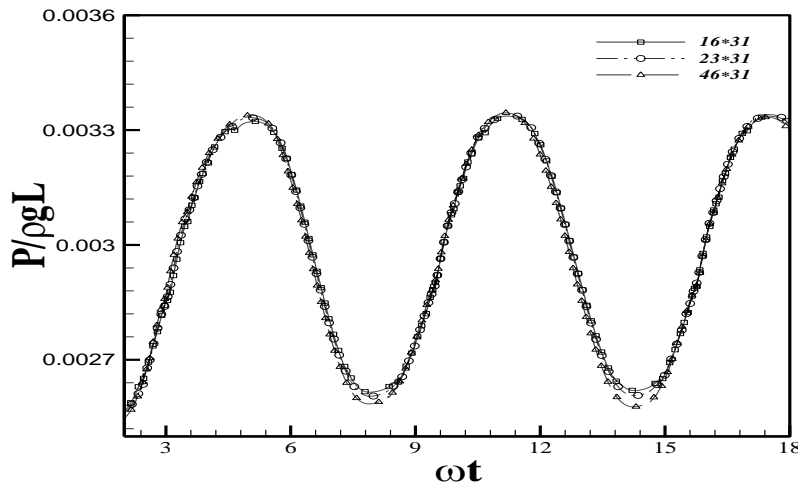


Figure 2. Time simulations of the pressure for three different grid systems at T1 for un-baffled tank. $h=0.31$ m; $\theta_0=4^0$; $\omega_R=2.0$ r/s.

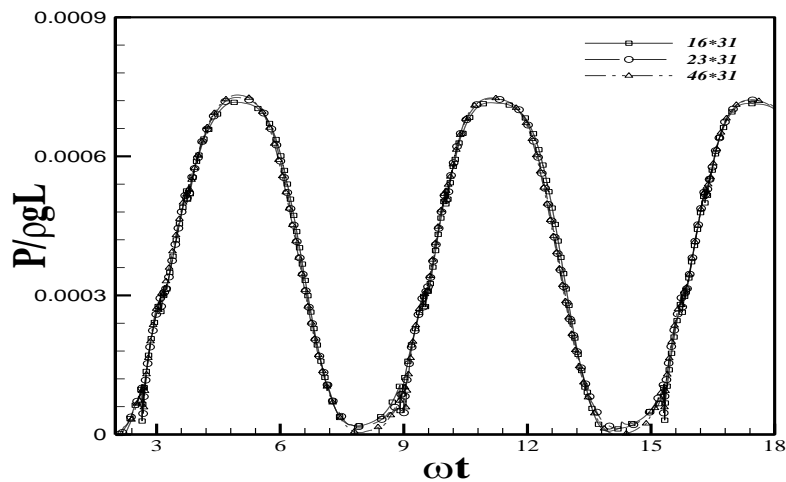


Figure 3. Time simulations of the pressure for three different grid systems at T3 for un-baffled tank. $h=0.465$ m; $\theta_0=4^0$; $\omega_R=2.0$ r/s.

When the period and amplitude of excitation are large, the liquid responds violently and causes the numerical solution to become unstable. The instability are related to the instability of the fluid motion, such as the occurrence of turbulence, wave breaking and the transition from homogeneous flow to a two-phase flow. For these situations, the present numerical model is limited to the period prior to the inception of these flow perturbations. On the other hand, in this study, to estimate the limited impact pressure on the tank top and to demonstrate the capability of the numerical code in computing impact-type loads, the slosh of liquid at 75% fill depth with the rolling amplitude 80 are chosen for all cases. Thus, the main purpose of this study is to assess numerically how the height of the baffle relative to the initial liquid depth affects the liquid sloshing. In order to denote validation, several comparisons have been made between the numerical solution and the experimental results available in the previous studies.

3. Results and discussions

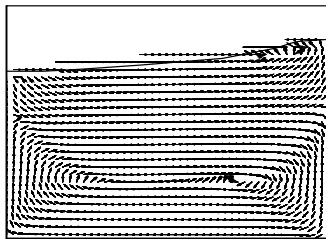
3.1 Free surface elevation

Fig. 4, Fig. 5, Fig. 6, Fig. 7, Fig. 8 and Fig.9 denote the snapshots of the liquid motion including the free surface deformation and the velocity at regular intervals during one period (T) of the rolling tank for different baffle heights. In the case of the unbaffled tank, the liquid sloshing is enough to reach to the top wall of the tank after impacting on the side walls of the tank as shown in Fig. 6(a-d). When the tank has the vertical baffle or the T-shape baffle with the height of $h_B / h = 0.2$ and $h_B / h = 0.4$, the pattern of liquid sloshing is almost similar to the case of the unbaffled tank as shown in Fig. 7(a-d) and Fig. 8(a-d). T-shape baffle represents the shallow water effects and the free surface behavior is getting stable slowly due to the wave breaking and the inertial forces. As the vertical baffle height increases continuously, the rolling motion of the liquid becomes slightly weaker due to the blockage effects of the baffles on the liquid convection. Additionally, the free surface behavior is getting stable and the inertial forces are not enough to propel the liquid to reach to the top wall of the tank as shown in Fig. 9, Fig. 10 and Fig. 11.

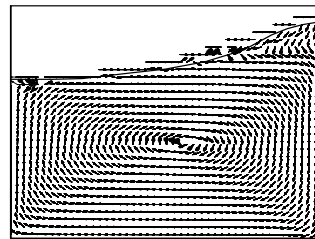
In the snapshots of the velocity vectors for one period (T) of the rolling motion of the tank for the various h_B / h , the velocity vectors near the left wall moves upward after the liquid impacts on the left wall. The vortex almost starts to form left behind the vertical baffle and T-shape baffle represents the shallow water effects. At this instant, the liquid shows the roof impact on the left top corner of the tank. This pattern is almost a reverse result when the tank moves right side.

As the vertical baffle height increases, the blockage effect of the vertical baffle on the liquid convection is predominant to the tip vortex. the strength of the vortex by liquid flow separation from the vertical baffle tip become weaker. The value of the maximum free surface elevation also keeps decreasing.

(a)



(b)



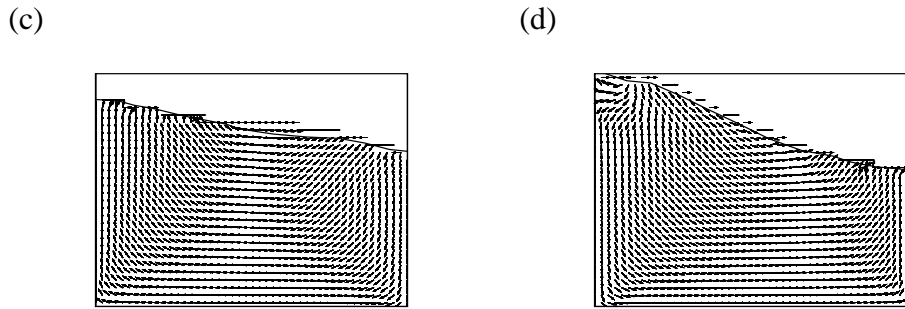
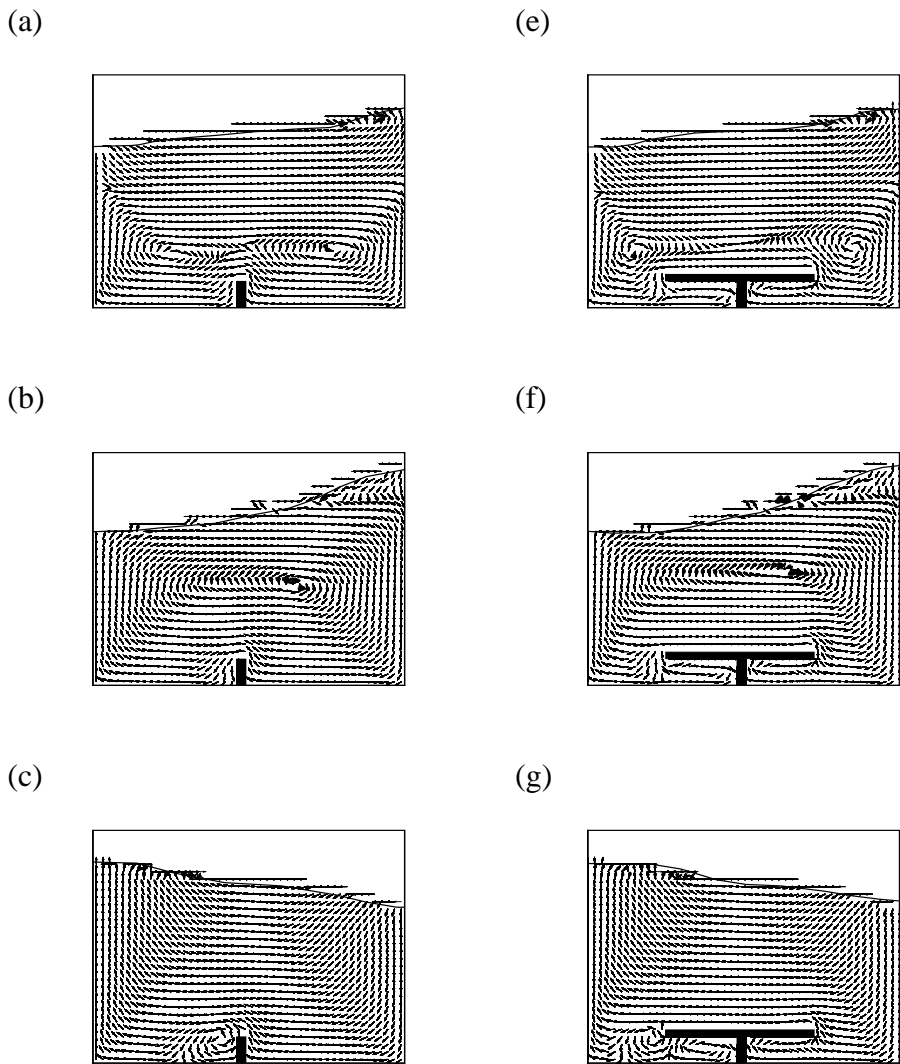


Figure 4. Snapshots of the velocity for one period (T) of the un-baffled tank motion, (a) $t = T/4$, (b) $t = T/2$, (c) $t = 3T/4$, (d) $t = T$, $\omega_R = 5.0$ r/s; $\theta_0 = 8^\circ$.



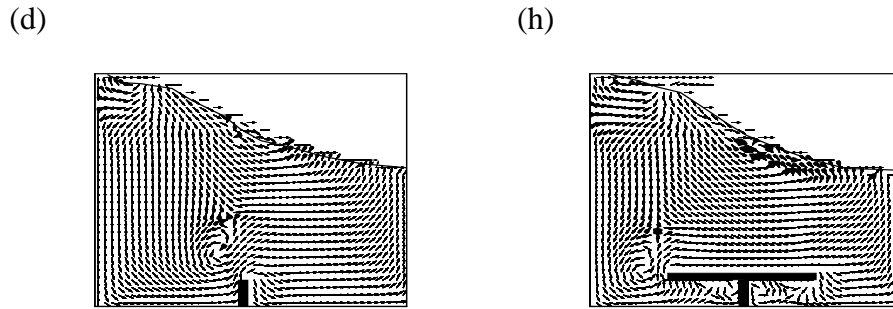
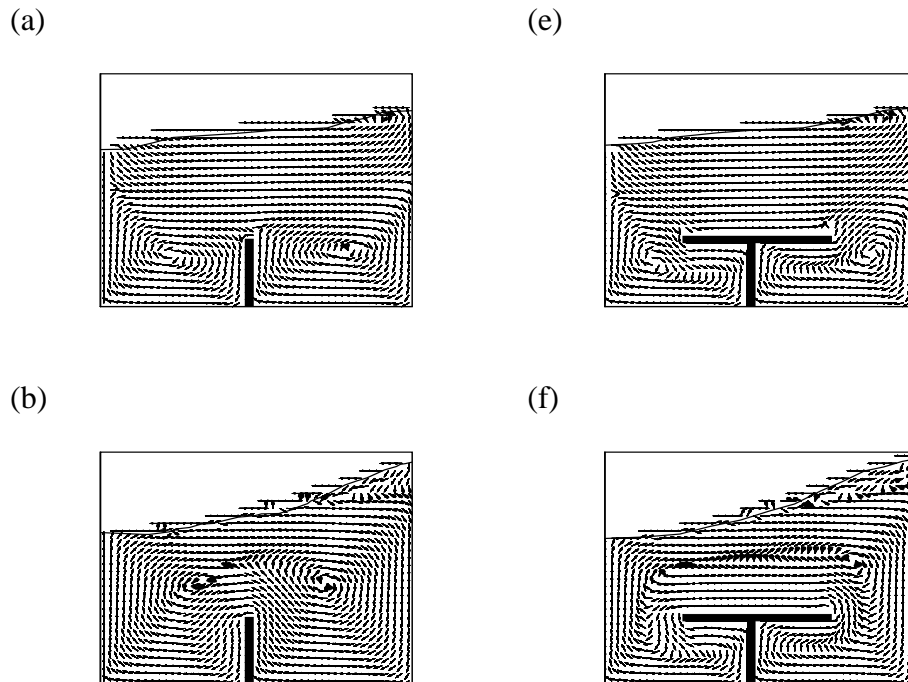


Figure 5. Snapshots of the velocity for one period (T) of the tank motion, $h_B / h = 0.2$, in the case of vertical baffle and in the case of T-Baffle. (a) $t = T/4$, (b) $t = T/2$, (c) $t = 3T/4$, (d) $t = T$, (e) $t = T/4$, (f) $t = T/2$, (g) $t = 3T/4$, (h) $t = T$, $\omega_R = 5.0$ r/s; $\theta_0 = 8^\circ$



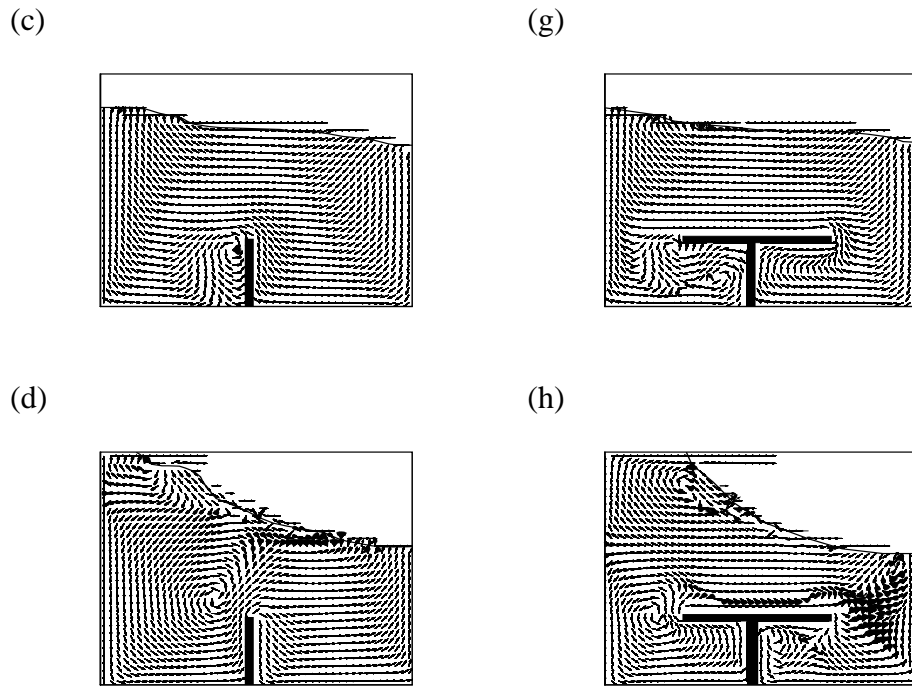
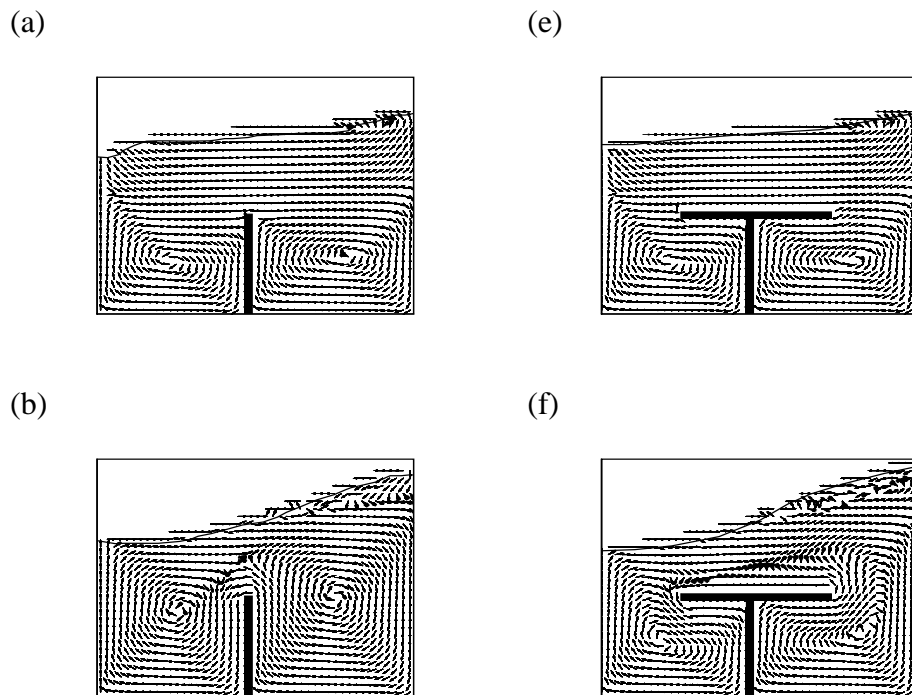


Figure 6. Snapshots of the velocity for one period (T) of the tank motion, $h_B / h = 0.4$, in the case of vertical baffle and in the case of T-Baffle. (a) $t = T/4$, (b) $t = T/2$, (c) $t = 3T/4$, (d) $t = T$, (e) $t = T/4$, (f) $t = T/2$, (g) $t = 3T/4$, (h) $t = T$, $\omega_R = 5.0$ r/s; $\theta_0 = 8^\circ$.



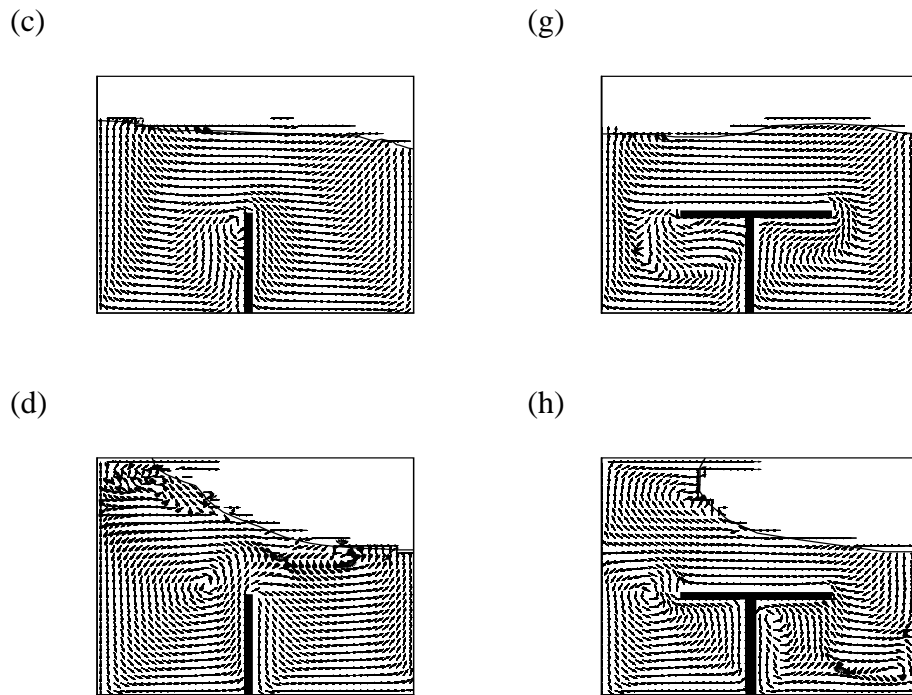
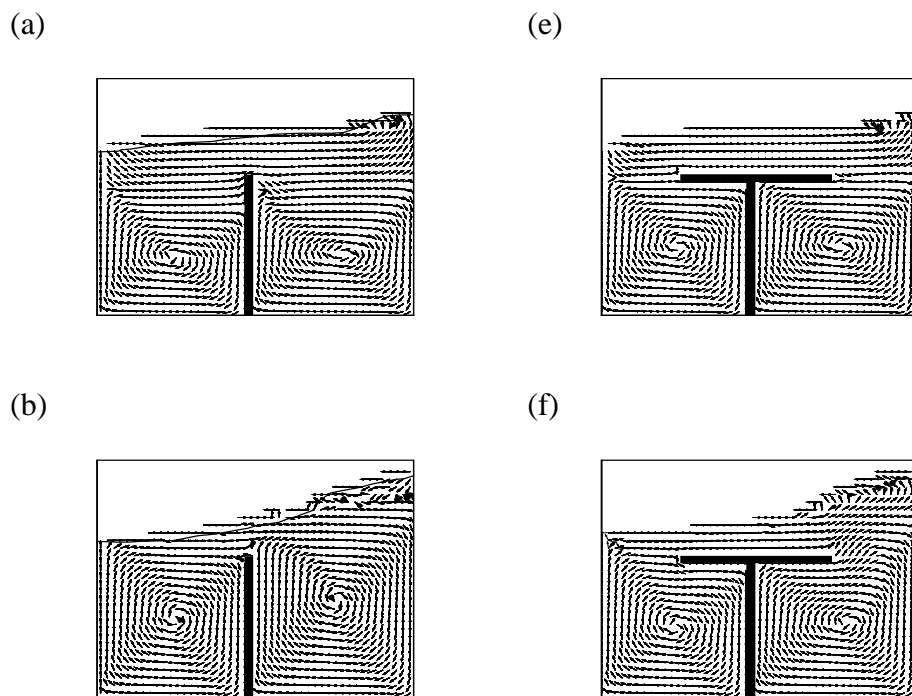


Figure 7. Snapshots of the velocity for one period (T) of the tank motion, $h_B / h = 0.6$, in the case of vertical baffle and in the case of T-Baffle. (a) $t = T/4$, (b) $t = T/2$, (c) $t = 3T/4$, (d) $t = T$, (e) $t = T/4$, (f) $t = T/2$, (g) $t = 3T/4$, (h) $t = T$, $\omega_R = 5.0$ r/s; $\theta_0 = 8^\circ$.



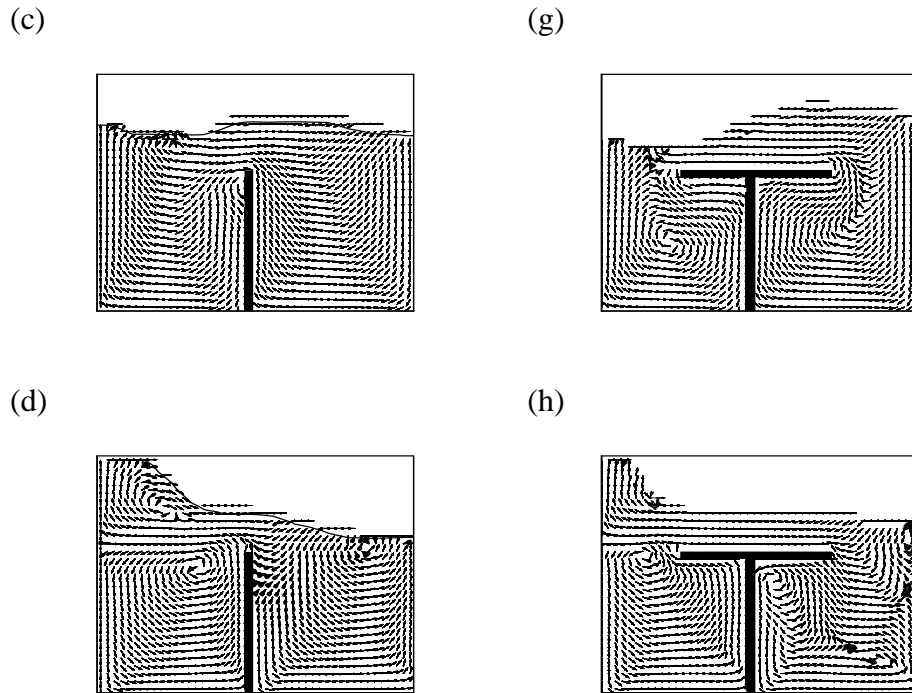
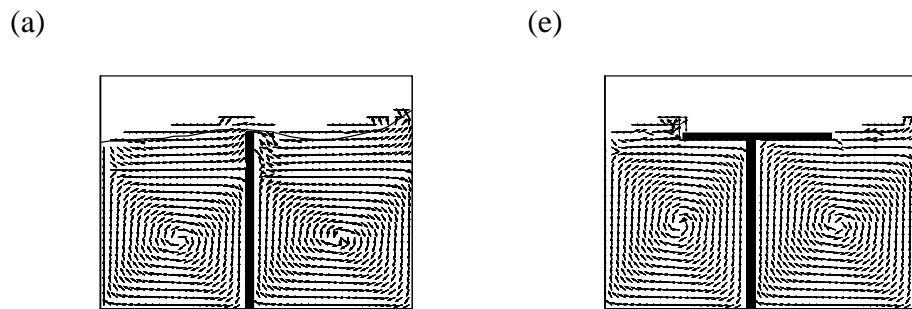


Figure 8. Snapshots of the velocity for one period (T) of the tank motion, $h_B / h = 0.8$, in the case of vertical baffle and in the case of T-Baffle. (a) $t = T/4$, (b) $t = T/2$, (c) $t = 3T/4$, (d) $t = T$, (e) $t = T/4$, (f) $t = T/2$, (g) $t = 3T/4$, (h) $t = T$, $\omega_R = 5.0$ r/s; $\theta_0 = 8^\circ$.



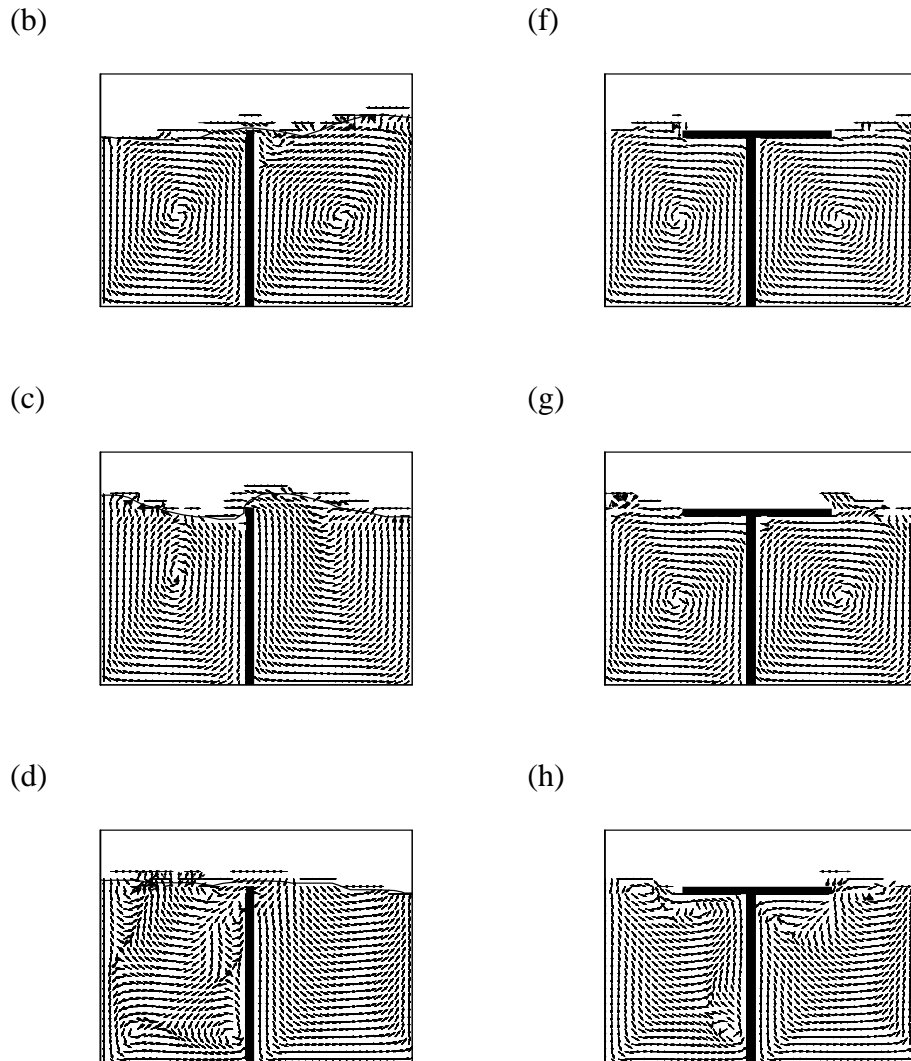


Figure 9. Snapshots of the velocity for one period (T) of the tank motion, $h_B / h = 1.0$, in the case of vertical baffle and in the case of T-Baffle. (a) $t = T/4$, (b) $t = T/2$, (c) $t = 3T/4$, (d) $t = T$, (e) $t = T/4$, (f) $t = T/2$, (g) $t = 3T/4$, (h) $t = T$, $\omega_R = 5.0$ r/s; $\theta_0 = 8^\circ$.

3.2 Wall pressures

The time simulations of the pressure due to the liquid sloshing at different transducers are presented in Fig. 10, Fig. 11, Fig. 12, Fig. 13, Fig. 14 and Fig. 15. In the cases of the vertical and T-shape baffled tank, except T4 for the un-baffled tank, the values of the pressure at T1, T2 and T3 behave almost periodically. At T4, the pressure is sensed when the roof impact occurs. At this probe, the roof impact of the liquid doesn't occur at any instant beyond the baffle height of $h_B / h \geq 0.65$. As h_B / h increases, the value of the maximum free surface elevation keeps decreasing and does not reach the top wall due to the suppression of the liquid sloshing by the hydrodynamic damping of the baffles.

It is of great importance to know the maximum pressure exerting on the tank wall in the design of the liquid tanks. Thus, the instantaneous peak values in the time histories of the pressure at each transducer have been averaged to obtain the mean maximum pressure according to the baffle height. Fig. 16 and Fig. 17 show the dependence of the mean maximum pressure on the baffle height. Since the transducers of T3 and T4 locate above the initial free surface height, the values of pressure at these transducers are obtained by net liquid impact, resulting in the dynamic pressures. As h_B/h and the rolling amplitude increase continuously, P_{max} diminishes rapidly. For smaller rolling amplitude (4°), the maximum pressures decrease slowly as shown in Fig. 16 and Fig. 17. The values of P_{max} for $h_B/h = 0.4$ and 0.8 are about 10% and 15 % less than that of $h_B/h = 0.0$ at T1 for the rolling amplitude 8° . On the other hand, the values of P_{max} for $h_B/h = 0.4$ and 0.8 are about 0.25% and 1% less than that of $h_B/h = 0.0$ at T1 for the rolling amplitude 4° . In the case of the vertical and horizontal baffles, the maximum pressures decrease approximately 6% more than that of the vertical baffle case and remain almost unchanged for all h_B/h (Fig. 17). P_{max} at T4 does not also reach the top wall due to the suppression of the liquid sloshing by the hydrodynamic damping and the shallow water effect of the T-shape baffle. In general, at T1, the static pressure is mainly predominant over the dynamic pressure. As h_B/h and the rolling amplitude increase continuously, P_{max} diminishes slowly for $h_B/h < 0.8$ and rapidly for $h_B/h \geq 0.8$. Then, It can be concluded that a vertical baffle for $h_B/h < 0.8$ would be more effective except the maximum dynamic pressure at T2 and T-shape baffle having a height $h_B/h \geq 0.8$ would be very effective in reducing the dynamic pressure.

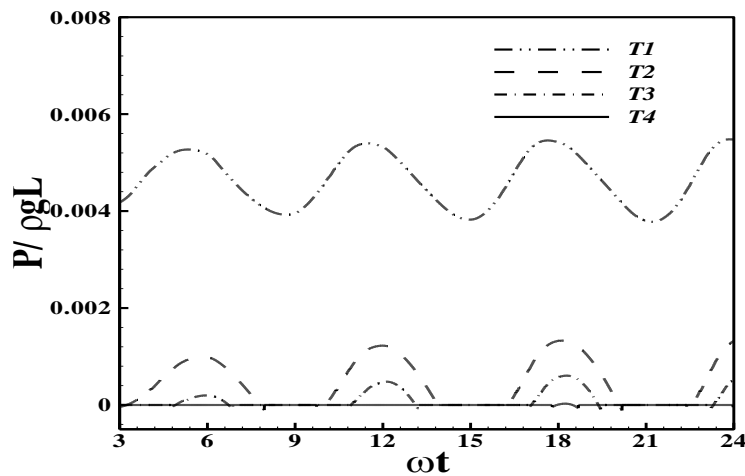


Figure 10. Pressure distributions at the transducers in T-baffled tank under the rolling motion. $h_B/h = 0.0$; $h = 0.465$ m; $\omega_R = 5.0$ r/s; $\theta_0 = 4^\circ$.

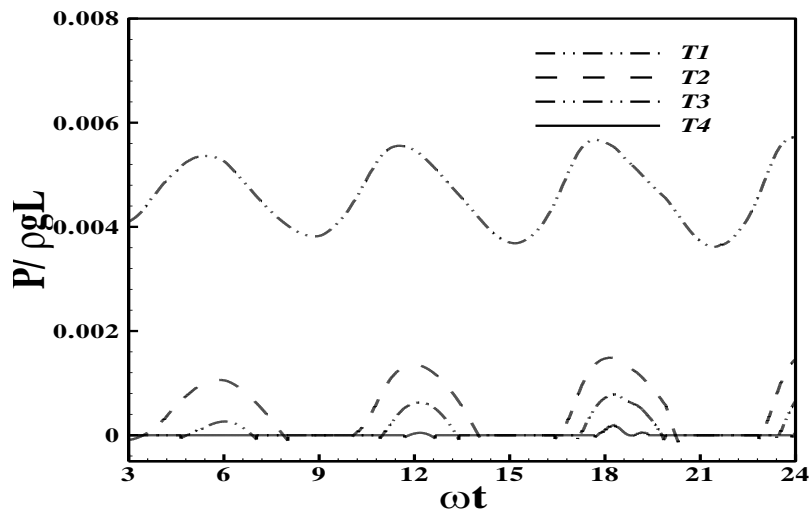


Figure 11. Pressure distributions at the transducers in T-baffled tank under the rolling motion. $h_B / h = 0.2$; $h = 0.465$ m; $\omega_R = 5.0$ r/s; $\theta_0 = 4^\circ$.

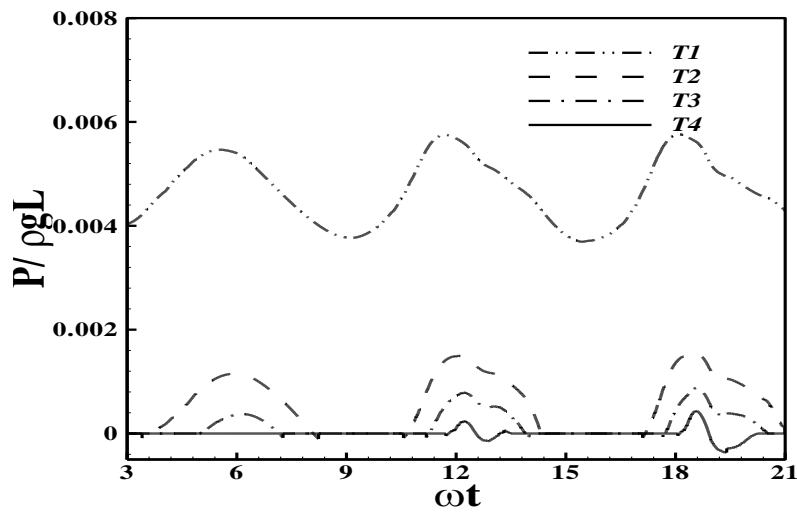


Figure 12. Pressure distributions at the transducers in T-baffled tank under the rolling motion. $h_B / h = 0.4$; $h = 0.465$ m; $\omega_R = 5.0$ r/s; $\theta_0 = 4^\circ$.

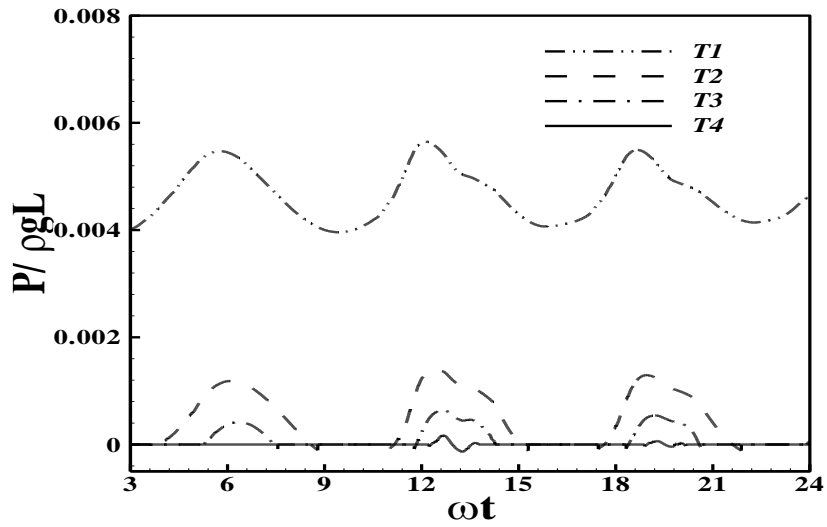


Figure 13. Pressure distributions at the transducers in a T-baffled tank under the rolling motion. $h_B / h = 0.6$; $h = 0.465$ m; $\omega_R = 5.0$ r/s; $\theta_0 = 4^\circ$.

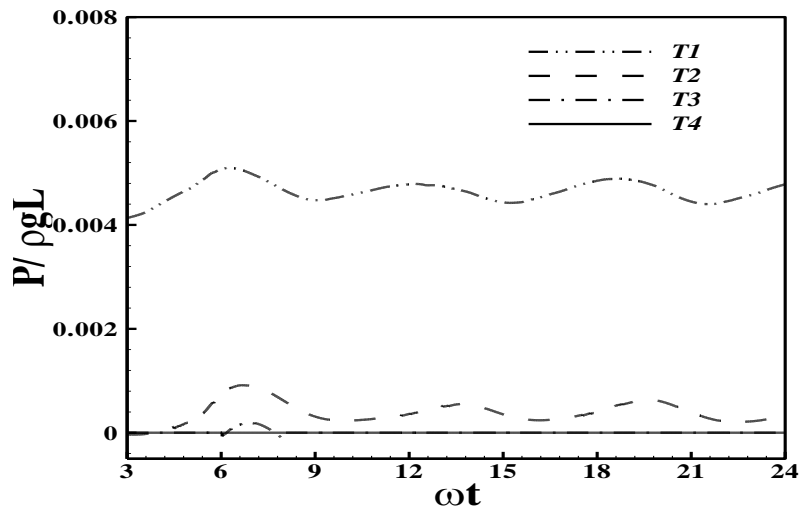


Figure 14. Pressure distributions at the transducers in a T-baffled tank under the rolling motion. $h_B / h = 0.8$; $h = 0.465$ m; $\omega_R = 5.0$ r/s; $\theta_0 = 4^\circ$.

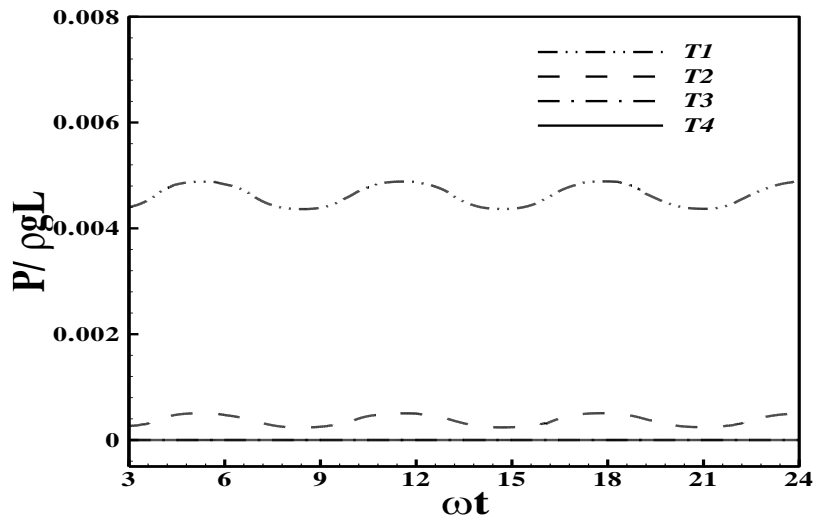


Figure 15. Pressure distributions at the transducers in a T-baffled tank under the rolling motion. $h_b/h = 1.0$; $h = 0.465$ m; $\omega_R = 5.0$ r/s; $\theta_0 = 4^\circ$.

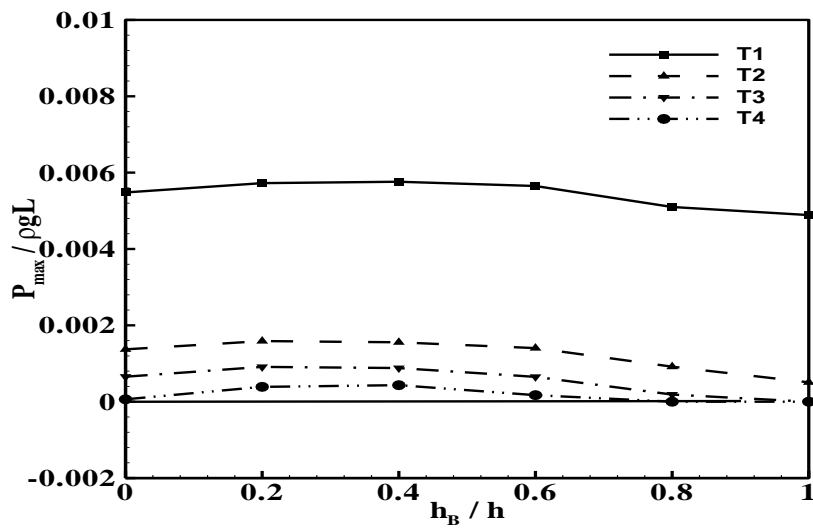


Figure 16. The mean maximum pressures in a T-baffled tank, $\theta_0 = 4^\circ$.

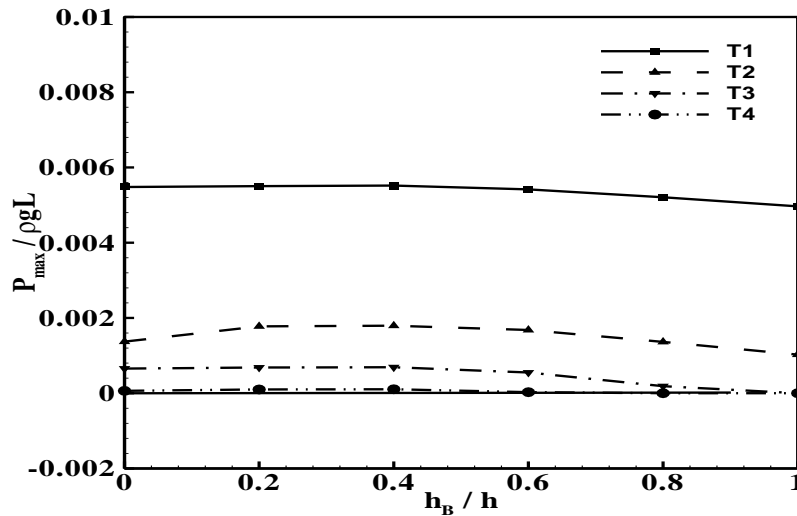


Figure 17. The mean maximum pressures in a vertical baffled tank, $\theta_0 = 4^0$.

4. Conclusions

In this study, the effects of the vertical baffle and the T-shape baffle are investigated based on the liquid sloshing in a moving partially filled 2D-rectangular tank. A numerical algorithm based on the volume of fluid technique (VOF) is used to study the non-linear behaviour of liquid sloshing. The numerical model solves the complete Navier-Stokes equations in primitive variables by using of finite difference approximations with the moving coordinate system. The ratio of the baffle height to the initial liquid depth has been changed in the range of $0 \leq h_B / h \leq 1.0$. For all cases, the fluid depth (h) is 75% of the tank height. The present time simulations of the pressure at T1 give a reasonable agreement with the experimental results of Akyildiz and Unal (2005), (2006). The little variations in the data are due to the ineptness of the experimental set up and the input parameters.

In the cases of the vertical and T-baffled tank, at T4, the roof impact of the liquid doesn't occur at any instant beyond the baffle height of $h_B / h \geq 0.65$. As h_B / h increases, the value of the maximum free surface elevation keeps decreasing and does not reach the top wall due to the suppression of the liquid sloshing by the hydrodynamic damping of the baffles including the blockage effects and the viscosity of baffle walls. The blockage effect of the vertical baffle on the liquid convection is predominant to the tip vortex and the strength of the vortex by liquid flow separation from the vertical baffle tip become weaker as h_B / h increases. The T-shape baffles also represent the shallow water effect and the inertial forces are not enough to propel the liquid to reach to the top wall of the tank. On the other hand, the maximum overturning moment for the T-baffled case would be much smaller.

Since the transducers of T3 and T4 locate above the initial free surface height, the values of pressure at these transducers are obtained by net liquid impact, resulting in the dynamic pressures. At T1, the static pressure is mainly predominant over the dynamic pressure. As h_B / h and the rolling amplitude increase continuously, P_{max} diminishes slowly for $h_B / h < 0.8$ and rapidly for $h_B / h \geq 0.8$. Then, It can be concluded that a vertical baffle for $h_B / h < 0.8$ would

be more effective except the maximum dynamic pressure at T2 and T-shape baffle having a height $h_B / h \geq 0.8$ would be very effective in reducing the dynamic pressure. Also seen is the fact that the maximum pressure at T2 installed at the still liquid surface, is less than that of the vertical baffle case due to the shallow water effect.

The effect of the vertical baffle is most pronounced in shallow water. It is revealed that flow over a vertical baffle produced a shear layer, and energy was dissipated by viscous action. On the other hand, the T-shape baffle is more effective in introducing the shallow water effects for deep water case which dissipated energy by forming a hydraulic jump and a breaking wave.

References:

- Armenio, V., Rocca, M.L., 1996. On The Analysis of Sloshing of Water in Rectangular Containers: Numerical Study and Experimental Validation, *Ocean Engineering*, 23(8), pp. 705-739.
- Akyildiz, H., Unal, E.N., 2005. Experimental investigation of pressure distribution on a rectangular tank due to the liquid sloshing, *Ocean Engineering*, 32, pp. 1503-1516.
- Akyildiz, H., Unal, E.N., 2006. Sloshing in a three dimensional rectangular tank: Numerical simulation and experimental validation, *Ocean Engineering*, 33(16), pp. 2135-2149.
- Celebi, M.S., Akyildiz, H., 2002. Nonlinear Modelling of Liquid Sloshing in a Moving Rectangular Tank, *Ocean Engineering*, 29(12), pp. 1527-1553.
- Chen, Y.G., Djidjeli, K., Price, W.G., 2009. Numerical simulation of liquid sloshing phenomena in partially filled containers, *Computers & Fluids*, 38, pp. 830– 842.
- Cho, J.R., Lee, H.W., 2004. Numerical study on liquid sloshing in baffled tank by nonlinear finite element method, *Computer Methods in Applied Mechanics and Engineering*, 193(23–26), pp. 2581–2598.
- Cho, J.R., Lee, H.W., Ha, S.Y., 2005. Finite element analysis of resonant sloshing response in a 2D baffled tank, *Journal of Sound and Vibration*, 228 (4–5), pp. 829–845.
- Eswaran, M., Saha, U.K., Maity, D., 2009. Effect of baffles on a partially filled cubic tank: Numerical simulation and experimental validation, *Computers and Structures*, 87, pp. 198– 205.
- Faltinsen, O.M., Timokha, A.N., 2009. *Sloshing*. Cambridge University Press, New York.
- Faltinsen, O.M., Timokha, A.N., 2001. An adaptive Multimodal Approach to Nonlinear Sloshing in a Rectangular Tank, *Journal of Fluid Mechanics*, 432, pp. 167-200.
- Ibrahim, R.A., 2005. *Liquid Sloshing Dynamics: Theory and Applications*. Cambridge University Press, New York.

- Godderidge, B., Tan, M., Earl, C., Turnock, S., 2006b. Multiphase CFD modelling of a lateral sloshing tank. In: Proceedings of the Ninth Numerical Towing Tank Symposium, Le Croisic.
- Godderidge, B., Tan, M., Earl, C., Turnock, S., 2007. Boundary layer resolution for modeling of a sloshing liquid. In: Proceedings of the Seventeenth Annual Conference of the International Society of Offshore and Polar Engineers, 3, pp. 1905–1911.
- Godderidge, B., Turnock, S., Tan, M., Earl, C., 2009a. An investigation of multiphase CFD modelling of a lateral sloshing tank, *Computers and Fluids*, 38, pp. 183–193.
- Godderidge, B., Turnock, S., Earl, C., Tan, M., 2009b. The effect of fluid compressibility on the simulation of sloshing impacts, *Ocean Engineering*, 36, pp. 578–587.
- Hirt, C.W., Nichols, B.D., 1981. Volume of fluid (VOF) method for the dynamics of free boundaries, *Journal of Computational Physics*, 39, pp. 201–225.
- Ibrahim, R.A., Pilipchuk, V.N., Ikeda, T., 2001. Recent Advances in Liquid Sloshing Dynamics, *Applied Mechanical Review* 54(2), pp. 133-199.
- Kim, Y., 2001. Numerical Simulation of Sloshing Flows with Impact Load, *Applied Ocean Research*, 23, pp. 53-62.
- Lee, D.H., Kim, M.H., Kwon, S.H., Kim, J.W., Lee, Y.B., 2007. A parametric sensitivity study on LNG tank sloshing loads by numerical simulations, *Ocean Engineering*, 34, 3–9.
- Liu, D., Lin, P., 2009. A numerical study of three-dimensional liquid sloshing in tanks, *Ocean Engineering*, 36, pp. 202–212.
- Pal, N.C., Bhattacharyya, S.K., Sinha, P.K., 2002. Non-Linear Coupled Slosh Dynamics of Liquid-Filled Laminated Composite Containers: a Two Dimensional Finite Element Approach, *Journal of Sound and Vibration*, 261(1), pp. 729-49.
- Pal, P., Bhattacharyya, S.K., 2010. Sloshing in partially filled liquid containers – Numerical and experimental study for 2-D problems, *Journal of Sound and Vibration*, 329, pp. 4466-4485.
- Panigrahy, P.K., Saha, U.K., Maity, D., 2009. Experimental studies on sloshing behavior due to horizontal movement of liquids in baffled tanks, *Ocean Engineering*, 36(3-4), pp. 213-222.
- Sames, P.C., Marcouly, D., Schellin, E.T., 2002. Sloshing in rectangular and cylindrical tanks, *Journal of Ship Research*, 46(3), pp. 186-200.
- Younes, M.F., Younes, Y.K., El-Madah, M., Ibrahim, I.M., El-Dannanh, E.H., 2007. An experimental investigation of hydrodynamic damping due to vertical baffle arrangements in a rectangular tank, *Proceedings of the Institution of Mechanical Engineers, Part M: Journal of Engineering for the Maritime Environment*, 221, pp. 115-123

